Nucleosynthesis of the Heavy Elements

Three basic processes can be identified by which heavy nuclei can be built by the continuous addition of protons or neutrons:

- p-process (proton)
- s-process (slow neutron)
- r-process (rapid neutron)

Capture of protons on light nuclei tend to produce only proton-rich nuclei. Capture of neutrons on light nuclei produce neutron-rich nuclei, but which nuclei are produced depends upon the rate at which neutrons are added. Slow capture produces nuclei near the valley of beta stability, while rapid capture (i.e., rapid compared to typical beta-decay timescales) initially produces very neutron-rich radioactive nuclei that eventually beta-decay towards the valley of beta stability. Some nuclei can be built by more than one process, as illustrated in Fig. 1.
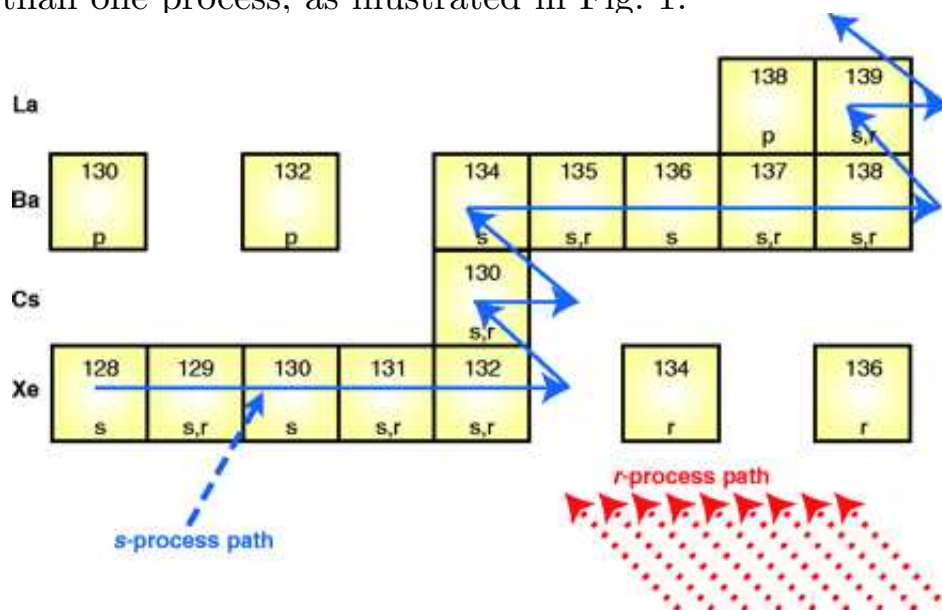

Figure 1: A small portion of the chart of the nuclides, illustrating isotopes built by the three basic processes. Only stable isotopes are shown, and letters indicate the processes that can contribute to these isotopes.

Neutron Capture

The difference between the s-process and r-process nucleosynthesis is controlled by beta decay rates of nuclei. The s-process path lies in the valley of beta stability, but the r-process path is shifted by many units toward neutron-richness. Fig. 2 shows the beta-decay timescales of radioactive neutron-rich nuclei, the positions of stable nuclei, neutron and proton magic numbers and the r-process path.
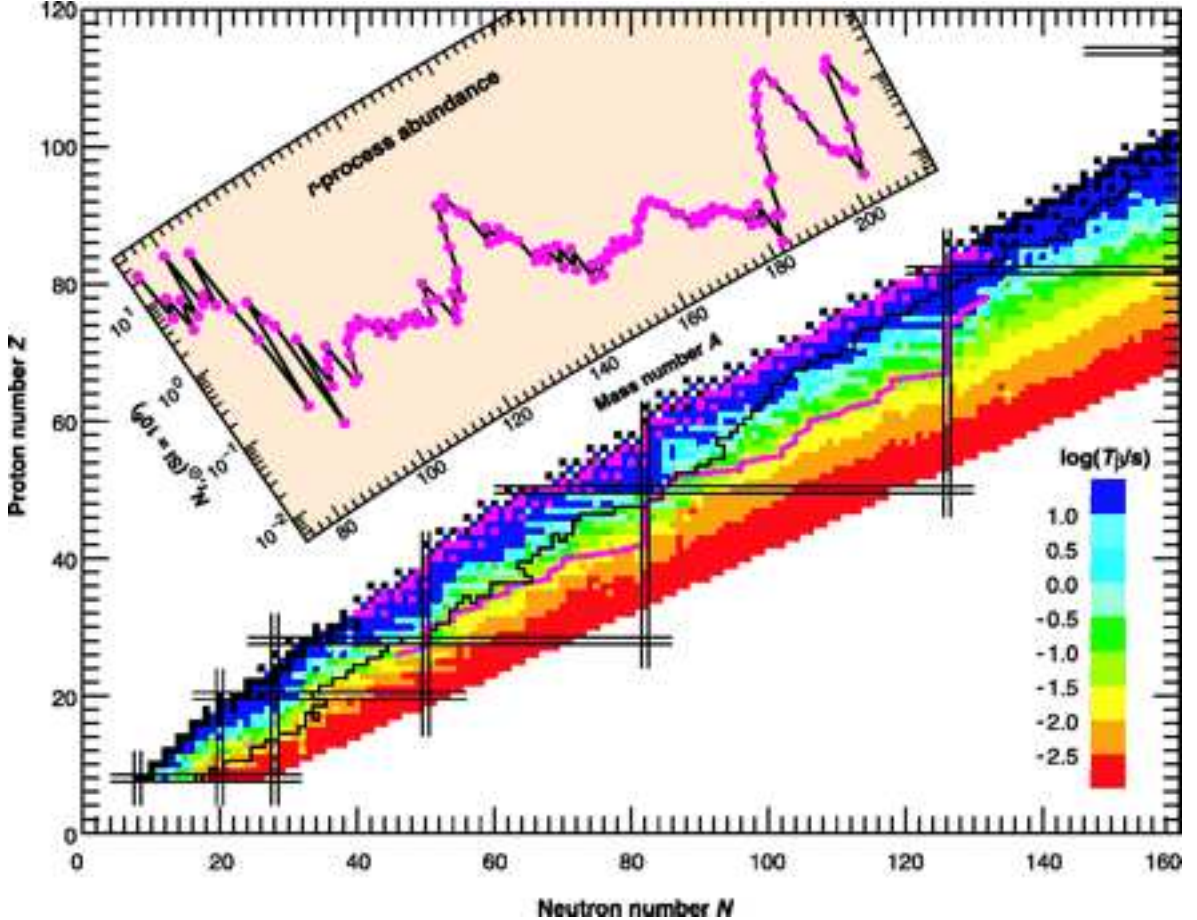

Figure 2: Chart of the nuclides illustrating beta decay timescales (color), stable isotopes (black squares), magic numbers (horizontal and vertical black lines), the limit of known nuclei (diagonal jagged black line), and the r-process path (purple line). Overlaid are the relative abundances of r-process nuclei, to illustrate the relation between magic numbers and abundances.

For small neutron velocities v, *i.e.,* energies up to a tens of keV, neutron capture cross sections vary as $\sigma \propto v^{-1}$. Thus the product σv is roughly

constant for thermal energies. Characteristic cross sections are about 100-1000 millibarns ($10^{-25} - 10^{-24}$ cm^2). For temperatures around 30 keV, thermal velocities of neutrons are about 3×10^8 cm s^{-3}. Then, the lifetime of a nucleus against neutron capture is

$$\tau_n \sim \frac{1}{n_n \sigma v} \sim \frac{3 \times 10^{16} - 3 \times 10^{17}}{n_n} \ \text{s}.$$

s-process timescales are around 10^4 yr, while r-process timescales are around microseconds, indicating neutron densities of $10^5 - 10^6$ cm^{-3} and $10^{23} - 10^{24}$ cm^{-3}, respectively. Neutron densities intermediate to these might be expected to yield a nucleosynthesis pattern intermediate to the s- and r-processes. However, comparison to solar-system abundances indicates that this has not occurred.

Neutron capture cross sections are generally smoothly varying with A because a captured neutron has an excitation energy of about 8 MeV ($\mu_n \simeq \mu_p \approx -8$ MeV) where the density of levels if very high. However, for light nuclei or magic number nuclei (N or $Z \in [2, 8, 20, 28, 50, 82, 126]$) this is not the case and the neutron capture cross section are very small, comparatively, being from 1 to 10 mb.

s-process

A quantitative analysis can be performed with the basic assumption that, except for magic number nuclei, beta decay timescales are all very rapid compared to the neutron cature rate. The nuclear chain thus indicated is unique, because one proceeds to heavier nuclei as indicated in Fig. 2, stepping horizontally until an unstable nucleus is reached, then moving on a diagonal path increasing the proton number by 1 and decreasing the neutron number by 1. One can let N_A represent the abundance of nucleus A with out reference to Z, and we can ignore abundances of radioactive nuclei. The differential equation for abundances is then

$$\dot{N}_A = - <\sigma v>_A n_n(t) N_A(t) + <\sigma v>_{A-1} n_n(t) N_{A-1}(t),$$

where $<\sigma v>_A$ is thermally averaged for each nucleus A. Under the assumption that $\sigma \propto v^{-1}$, one can write $<\sigma v>_A \approx v_T \sigma_A$ where v_T is the thermal velocity which is a constant. Defining a *neutron exposure* τ by

$$d\tau = v_T n_n(t) \, dt,$$

we find
$$N'_A = -\sigma_A N_A + \sigma_{A-1} N_{A-1}.$$

This equation can only be solved with a suitable boundary condition. Because neutron capture cross sections on light nuclei are so small, we can effectively assume that $N_A(0) = 0$ for $A < 56$ and $N_A(0) = N_{56}(0)$ for $A > 56$. On the other hand, for $A = 209$ the chain cerminates because Bi^{209} is the most massive stable nucleus. Nuclei with mass 210 decay by α decay to mass 206. We will ignore this complication.

The above equation has the property that $N'_A < 0$ if $N_A > (\sigma_{A-1}/\sigma_A)N_{A-1}$ and vice-versa. Thus it is self-regulating: N_A decreases if it is too large with respect to N_{A-1} and increases if it is too small. If the process operates long enough, it will come to equilibrium: $N_{A'} = 0$, in which case

$$\sigma_A N_A \approx \sigma_{A-1} N_{A-1}.$$

In-between the magic numbers, the cross sections are large compared to their differences, so locally this is a good approximation to the solution.

Over a large range of A, however, this result is a poor approximation, because of the small cross sections associated with magic nuclei. A proper general soution is a little tricky, but can be analyzed by using the Laplace transform

$$\hat{N}_k(s) = \int_0^\infty N_k(t) e^{-st} dt$$

using $k = A - 55$. Using the fact that the Laplace transform of a derivative is

$$\int_0^\infty N'_k(t) e^{-st} dt = s\hat{N}_k(s) - N_k(0),$$

the transformed equations and boundary condition are:

$$s\hat{N}_1(s) = -\sigma_1 \hat{N}_1(s) + N_1(0),$$
$$s\hat{N}_k(s) = -\sigma_k \hat{N}_k(s) + \sigma_{k-1}\hat{N}_{k-1}(s).$$

The solution of these equations, by substitution, is

$$\hat{N}_k(s) = \frac{N_1(0)}{\sigma_k} \prod_k \frac{\sigma_k}{s + \sigma_k}.$$

Here the notation Π_k indicates successive multiplications of arguments from subscript k to 1. Since the product σN is expected to be smoothly varying,

we choose to use that product as the dependent variable. We define

$$\hat{\psi}_k(s) \equiv \frac{\sigma_k \hat{N}_k(s)}{N_1(0)} = \prod_k (1 + s/\sigma_k)^{-1}.$$

The solution is then the inverse Laplace transform:

$$\psi_k(\tau) \equiv \sigma N_k(\tau) = \frac{1}{2\pi i} \int_{-i\infty}^{i\infty} \hat{\psi}_k(s) e^{s\tau} ds$$

$$= \sum_{i=1}^{k} e^{-\sigma_i \tau} \sigma_i \prod_{k \neq i} \frac{\sigma_k}{\sigma_k - \sigma_i}.$$
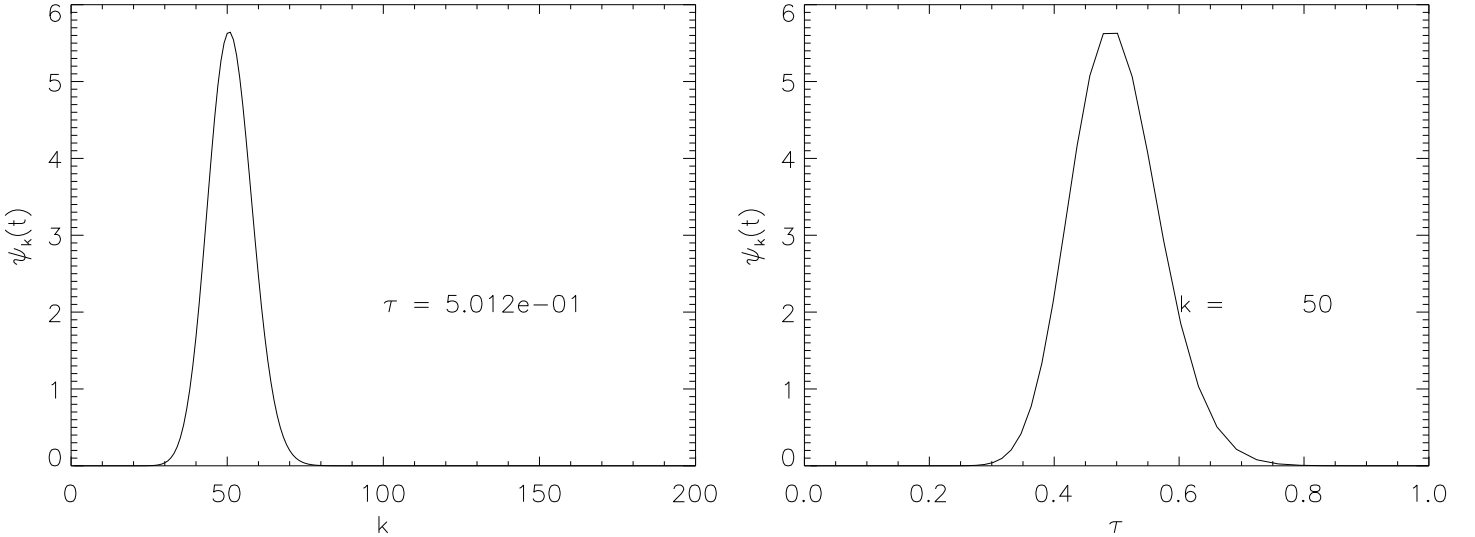

Figure 3: The distribution function $\psi_k(\tau)$ using $\sigma = 100$. Left: Shown as a function of k for $\tau = 0.5012$. Right: Shown as a function of τ for $k = 50$.

This solution encounters severe numerical difficulties at large atomic weights. The sum must be taken over about 150 terms, which differ greatly in order of magnitude but still must be included because of their near cancellations. It is therefore necessary to find an approximate solution. To illustrate the behavior of the exact solution, consider the idealized case in which all the cross sections are equal, $\sigma_k = \sigma$. The solution in that case, starting from

$$\hat{\psi}_k(s) = (1 + s/\sigma)^{-k},$$

is

$$\psi_k\left(\tau\right) = \frac{\sigma}{(k-1)!}\left(\sigma\tau\right)^{k-1}e^{-\sigma\tau},$$

which is a Poisson-like distribution in both k and τ with maxima at $k_{max} = \sigma\tau + 1$ and $\tau_{max} = \sigma^{-1}(k-1)$. Thus, as the neutron exposure τ increases, the maximum in the distribution moves to larger values of k. The abundance (distribution width) at the maximum $N_{k_{max}} = \Delta_{k_{max}}^{-1} \simeq (2\pi\sigma\tau)^{-1/2}$ decreases (increases) with k.

The approximate solution begins with this result. If we can find numbers λ_k and m_k such that

$$\left(1 + \frac{s}{\lambda_k}\right)^{-m_k} \simeq \Pi_k\left(1 + \frac{s}{\sigma_k}\right)^{-1}$$

for small s, we could write an approximate solution in the general case as

$$\psi_k\left(\tau\right) \simeq \lambda_k\frac{(\lambda_k\tau)^{m_k-1}}{\Gamma\left(m_k\right)}e^{-\lambda_k\tau}.$$

It can be shown that the constraint that the first three moments of $\psi_k(\tau)$ for the approximate case equal that of the general case, *i.e.*,

$$\int_0^\infty \psi_k\left(\tau\right)d\tau = 1,$$

$$\int_0^\infty \tau\psi_k\left(\tau\right)d\tau = \sum_i^k \sigma_i^{-1},$$

$$\int_0^\infty \tau^2\psi_k\left(\tau\right)d\tau = \left(\sum_i^k \sigma_i^{-1}\right)^2 + \sum_i^k \sigma_i^{-2},$$

yields

$$m_k = \frac{\left(\sum_{i=1}^k \sigma_i^{-1}\right)^2}{\sum_{i=1}^k \sigma_i^{-2}}, \qquad \lambda_k = \frac{\sum_{i=1}^k \sigma_i^{-1}}{\sum_{i=1}^k \sigma_i^{-2}}.$$

This solution is valid to better than 10% accuracy, which is small compared to the numerical uncertainty in the experimental products $\sigma_k N_k$.

Each function $\psi_k(\tau)$ begins at zero, rises to a single maximum at some value $\tau_{k,max}$ and then falls exponentially to zero at large τ. Magic numbers

produce abrupt changes in the distributions. Often, results are expressed in terms of the number of neutrons captured per initial iron seed nucleus instead of τ, a relationship which depends upon the values of the cross sections in the capture chain.
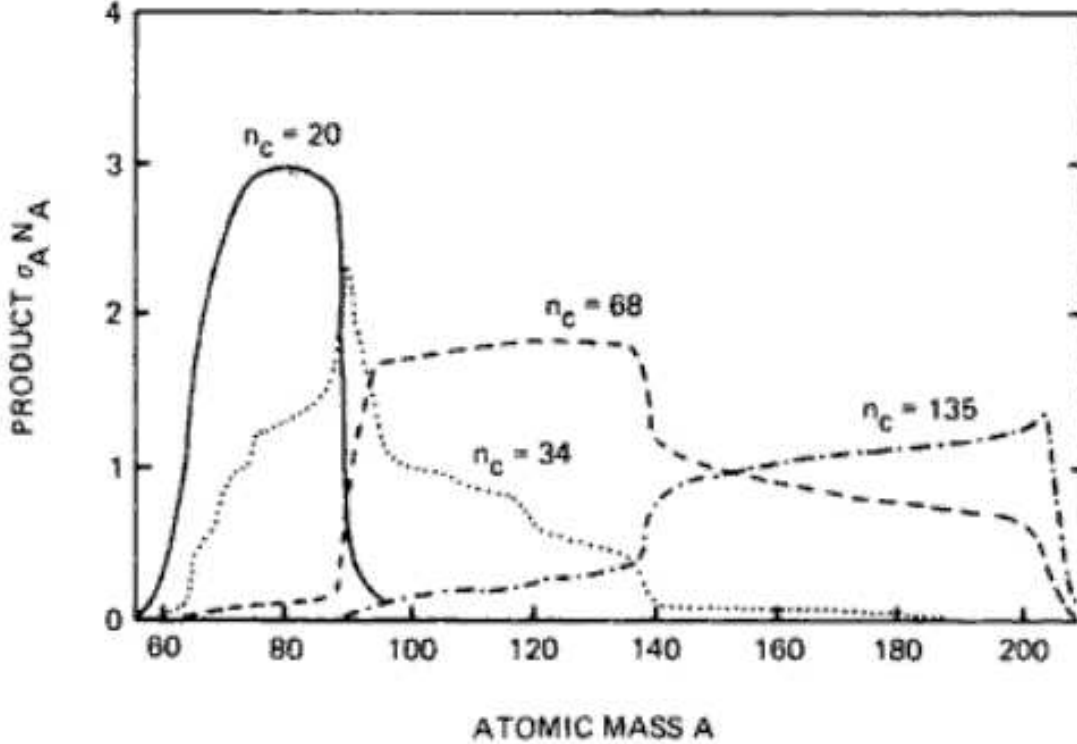

Figure 4: The distribution function ψ_A for different labels of total neutron irradiation, labelled by n_c, the average number of neutrons captured per initial seed nucleus (Fe).

Each s-process event results in a different abundance pattern because the exposure τ varies from event to event. An often-used approximation is that the probability of an event is equal to $Ge^{-\tau/\tau_o}$ with G and τ_o parameters. With this approximation, the abundance patter produced overall will be

$$\sigma_A N_A \simeq \int_0^\infty G\lambda_A e^{-\tau/\tau_o}\frac{(\lambda_A\tau)^{m_A-1}}{\Gamma(m_A)}e^{-\lambda_A\tau}d\tau = G\left(\frac{\lambda_A\tau_o}{1+\lambda_A\tau_o}\right)^{m_A}.$$

That such a simple model accurately reproduces solar system s-process abundances is taken as confirmation of the general correctness of the ideas.
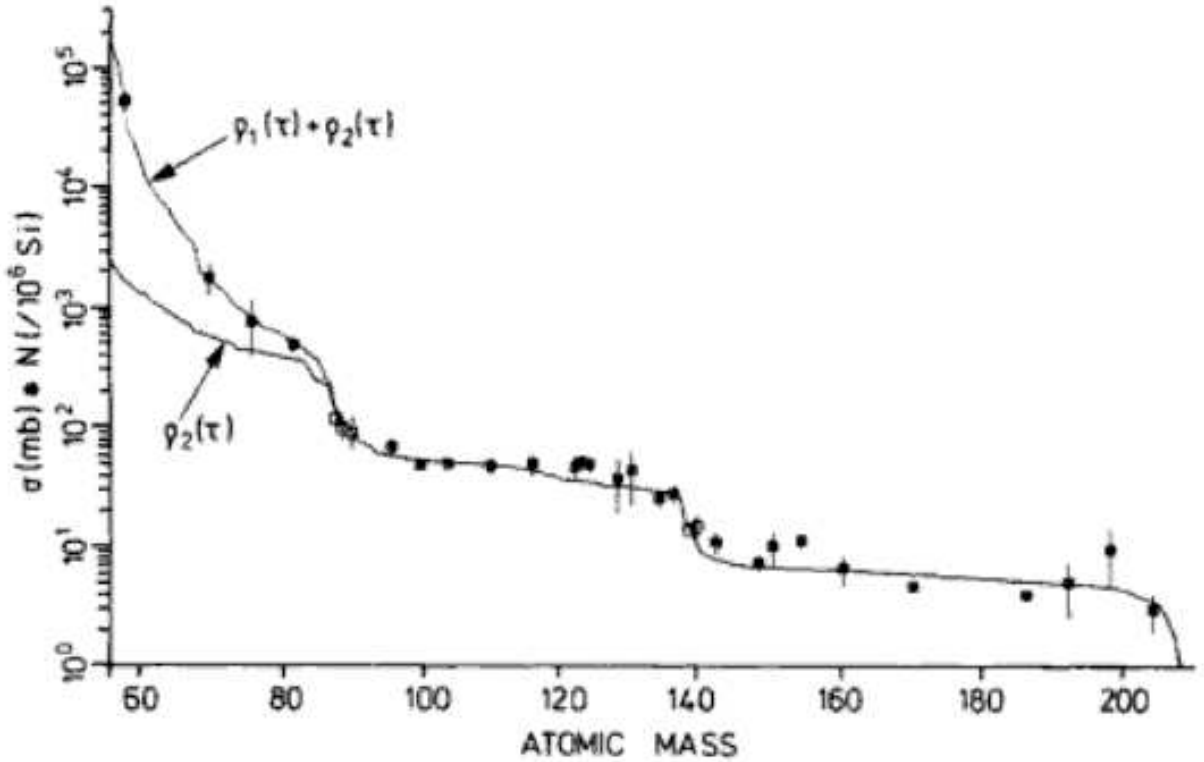
Figure 5: The solar system s-process abundances. The two curves show theoretical calculations for a single exponential distribution of neutron exposures ($\rho_2(\tau)$) and for a double exponential distribution with different timescales ($\rho_1(\tau) + \rho_2(\tau)$).

r-process

Extraction of the r-process abundances requires removal of the contribution from the s-process. However, the s-process abundances are well-fit by a smoothly varying function as described above, so the r-process abundance pattern can be reliably extracted. It is shown in Fig. 1, and compared to the s-process abundances in Fig. 6.

In comparison the s-process, we can make the assumption that the beta-decay timescale is long compared to the neutron capture timescale. In this case, the capture chain continues at fixed Z until one goes so far from the path of beta stability, and the neutron binding energy becomes so low (practically zero), that further neutron captures are rejected. Then, for each charge Z, there will be a *waiting point* at which a beta decay must occur in order to continue the chain to larger A. The abundance at each charge Z is governed then by

$$\dot{n}_Z(t) = \lambda_\beta^{Z-1} n_{Z-1}(t) - \lambda_\beta^Z n_Z(t),$$
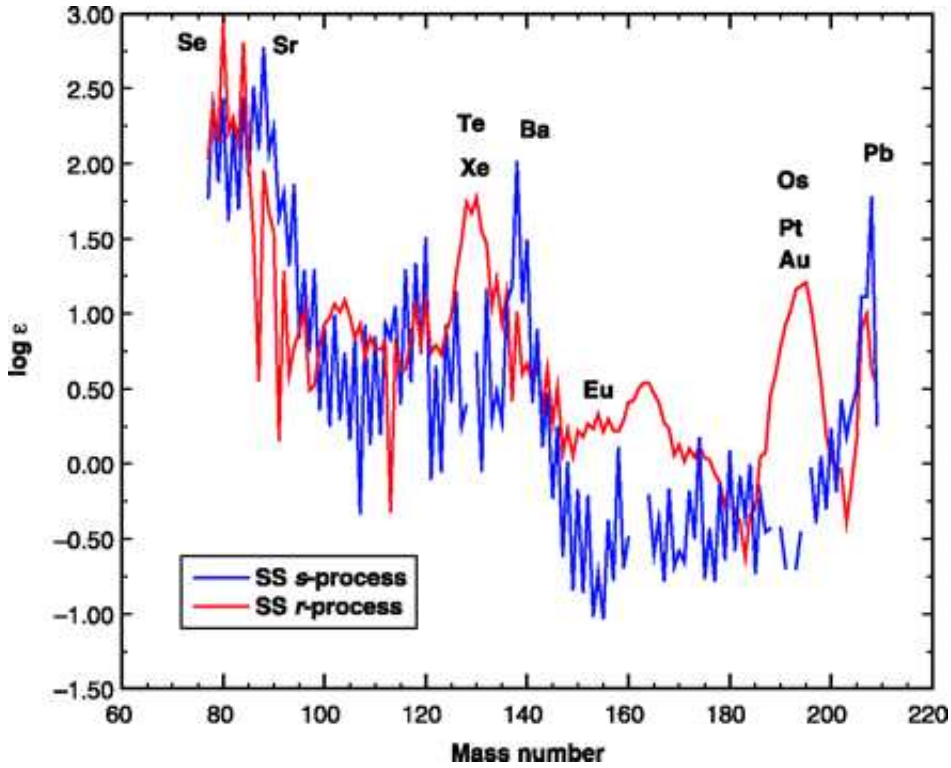
Figure 6: Comparison of s- and r-process abundances from solar system (meteoritic) data.

where λ_β^Z is the beta-decay rate at the waiting point for charge Z. The formal solution of these equations is like that of the s-process, except that abundances are inversely proportional to the beta-decay rate rather than the neutron-capture rate. Presumably, the slowest beta-decays will be in conjunction with magic numbers, so the highest abundances will thus be associated with magic numbers. Since nuclei eventually beta decay to the valley of beta stability once the r-process is over, the highest abundances of r-process nuclei will be shifted to lower N than the magic neutron numbers, as is indeed observed in Fig. 1.

Another feature is that the neutron density and the temperature play an important role in determining the position of the waiting points. The greater the neutron density and the lower the temperature, the more neutron-rich the waiting points and the r-process capture path will be. To reproduce solar system r-process abundances implies a fixed relation between these quantities. It is fascinating the the r-process abundance pattern in very old stars (Fig. 7) is very similar to that of the solar system. This implies that

there might be one dominant source for the r-process and that this source has not changed significantly over cosmic history.
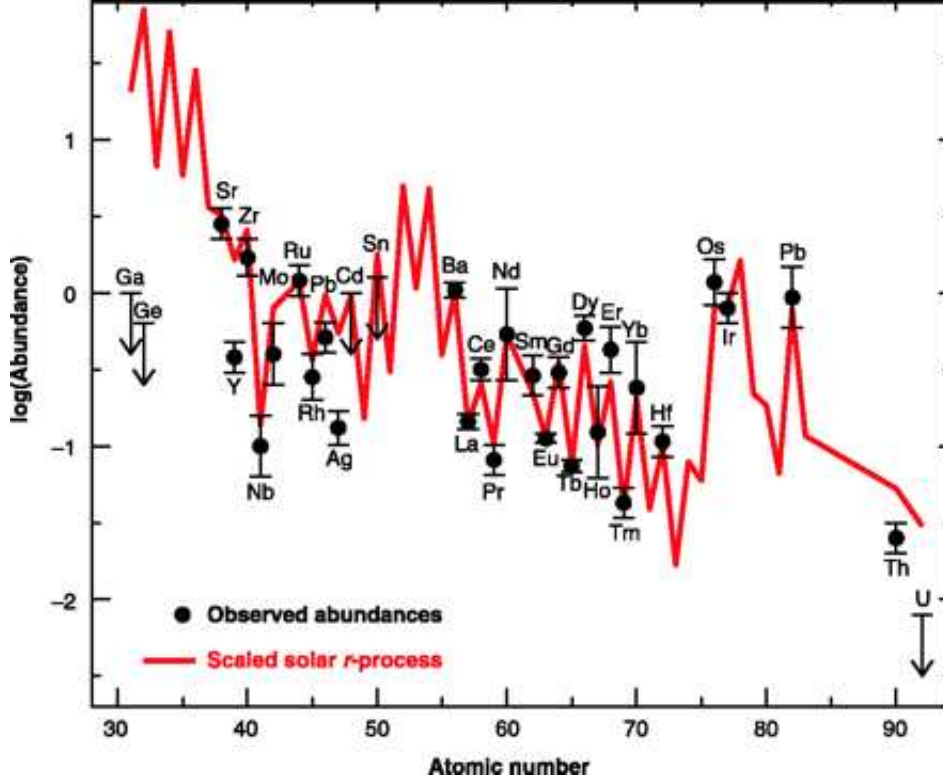

Figure 7: Abundance comparison between the ultra metal-poor halo star CS 22892-052 (points with bars) to scaled solar system r-process abundances (curve).

We also examine a simple steady-flow model, which should be valid in the limit of very high neutron abundances, in which fissions and photo-disintegrations are disregarded. The only operative processes are beta decays and neutron captures. The evolution of nucleus (Z, A) is

$$
\frac{dN(Z, A)}{dt} = \lambda_n^{Z, A-1} N(Z, A-1) + \lambda_\beta^{Z-1, A} N(Z-1, A)
$$
$$
- \lambda_n^{Z, A} N(Z, A) - \lambda_\beta^{Z, A} N(Z, A).
$$

Note our change of notation $\lambda_n^{Z, A-1} = \sigma_{A-1}$. Now sum over all the isobars of an isobaric chain A, for which the abundance is $N(A)$:

$$
\frac{dN(A)}{dt} = \lambda_n^{A-1} N(A-1) - \lambda_n^A N(A),
$$

where

$$\lambda_n^A = \sum_{Z \geq Z_{min(A)}} \lambda_n^{Z,A} \frac{N(Z,A)}{N(A)}.$$

The ratio $N(Z,A)/N(A)$ is the contribution of nucleus (Z,A) to the isobaric chain A, and is a function of the branching ratio between its β-decay and neutron capture probabilities:

$$\frac{N(Z,A)}{N(A)} = \frac{\lambda_\beta^{Z,A}}{\lambda_n^{Z,A} + \lambda_\beta^{Z,A}}.$$

Then, the steady state solution of the above is

$$N(A) = \frac{N_0}{\lambda_n^A} = N_0 \left(\sum_Z \frac{\lambda_\beta^{Z,A} \lambda_n^{Z<A}}{\lambda_\beta^{Z,A} + \lambda_n^{Z,A}} \right)^{-1},$$
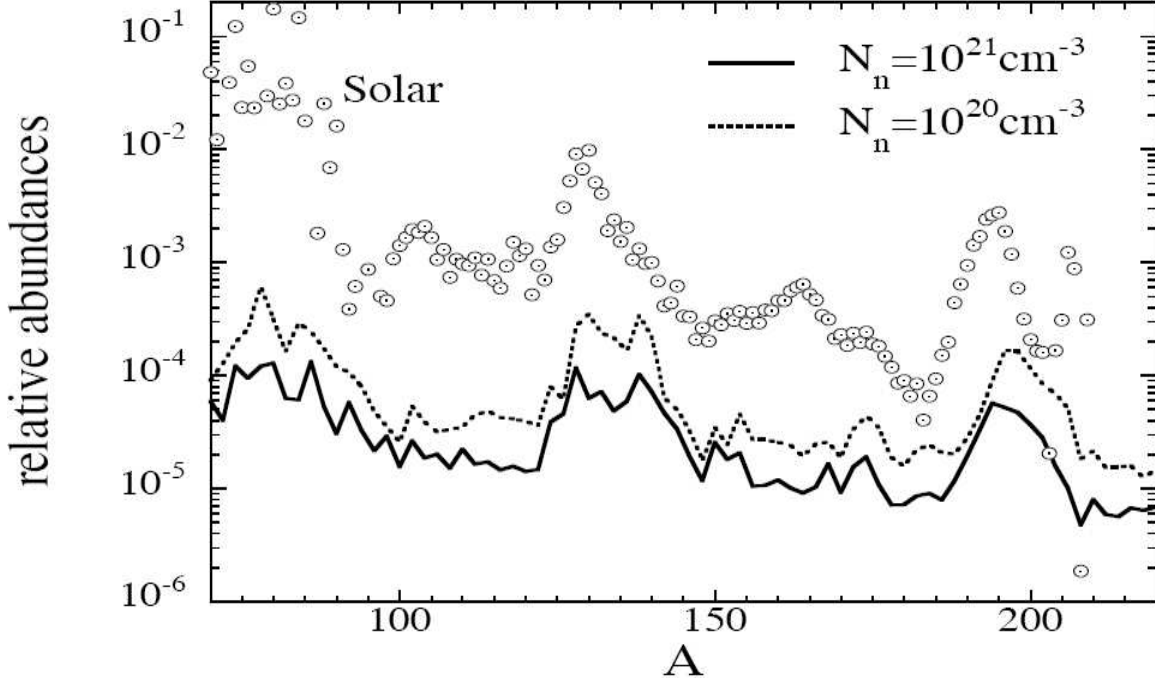
where N_0 is a normalization constant.

Figure 8: Comparison of r-process abundances from solar-system meteoritic data with the high-density neutron flow approximation.

The source of the r-process is not a settled question. The two competing sites are in Type II supernova and in the mergers of neutron stars with other neutron stars or black holes in compact binaries. While the latter site seems more speculative, we do no that such compact binaries exist and that mergers will occur on timescales as short as 10 million years, comparable to the lifetimes of very massive stars responsible for Type II supernovae. Models have indicated that mergers could result in the ejection of hundredths of a solar mass of neutron star matter, which upon its decompression, will produce r-process nuclei.

Supernovae have a difficulty in that their ejecta does not seem to be sufficiently neutron-rich to drive an effective r-process, at least one capable of producing nuclei associated with the last neutron magic number. The problem is that the prodiguous neutrinos emitted from the proto-neutron star on the several second timescale associated with the r-process have nearly equal fluxes of neutrinos and anti-neutrinos. This means that neutrino capture reactions tend to equilibrate the neutron and proton number densities, preventing a large neutron excess from developing. However, an advantage to the supernova site is that only a very small mass of r-process nuclei, about 10^{-5} $M_\odot$ per explosion, would be required to yield solar system abundances. Mergers require about 0.01 $M_\odot$ or more per merger.

p-process

There are 32 stable proton-rich nuclei which are shielded against neutron capture that can be found in nature. While the p-process possibly occurs in Type II supernova explosions, accretion onto neutron star surfaces resulting in Type I X-ray bursts has been shown to produce some of these nuclei as well. Furthermore, observed timescales of these bursts bear good relationship to expected p-process timescales.

Nuclear Cosmochronology

There are several long-lived isotopes that can be used to model the history of nucleosynthesis in the universe. These include I^{129} (0.0169), Pu^{244} (0.082), U^{235} (0.713), U^{238} (4.51), Th^{232} (13.9) and Re^{187} (40.), where the half-lives are given in Gyr in parentheses. The first two have half lives so short that no detectable quantites exist today, but their presence in the early solar system can be inferred from anomalies of isotopic abundances into which they decay. The other nuclei occur in the Earth and in meteorites. It is generally assumed nucleosynthesis occurred over a period of time T roughly equal to the age of the galaxy or its disc. So $T \sim 10$ Gyr. This duration T is followed by an interval ΔT, of order 10^8 yr, which represents the time required for the solidification of the solid bodies in the solar system (i.e., meteorites). During ΔT, all radioactivities decay exponentially, and the extinct radioactivities are measured by the amounts of xenon gas into which they decay that is trapped within the meteorites. Note that each of these radioactive isotopes are produced by the r-process.

Consider the two U isotopes. The relative abundances today of 235/238 is 0.00723, and cannot have been affected by chemical processes. So the isotopic ratio 4.6 Gyr ago was about 0.31. If all the U was produced in a single event, with a production ratio R estimated to be between 1.4 and 1.8, this yields a time

$$T = (\lambda_{238} - \lambda_{235})^{-1} \log \left(\frac{N_{238}}{R N_{235}} \right) \simeq 2.5 \text{ Gyr}$$

or a total age of about 7 Gyr. On the other hand, if the production of U isotopes has proceeded uniformly, then

$$\frac{N_{235}}{N_{238}} = R \frac{\lambda_{235}}{\lambda_{238}} \left(\frac{e^{-\lambda_{238} T} - 1}{e^{-\lambda_{235} T} - 1} \right) \simeq 10 \text{ Gyr,}$$

or production started about $T + 4.6$ Gyr $= 15$ Gyr ago. (Note $e^{-\lambda \tau_{1/2}} = 1/2$, or $\lambda = \tau_{1/2}^{-1} \ln 2$.) These two approximations bracket all realistic models.

Suppose the production rate of r-process isotopes decreases as $e^{-\Lambda t}$ over the interval T, so that $\Lambda = 0[\infty]$ corresponds to uniform [sudden] nucleosynthesis. Then, the ratio of two isotopes after a time T is

$$\frac{N_A}{N_B}(t) = R \left(\frac{\Lambda - \lambda_A}{\Lambda - \lambda_B} \right) \left(\frac{e^{(\Lambda - \lambda_B) T} - 1}{e^{(\Lambda - \lambda_A) T} - 1} \right).$$